Journal of Sound and Vibration (2001) **241**(5), 809–824
doi:10.1006/jsvi.2000.3333, available online at http://www.idealibrary.com on IDEAL®

RESPONSE OF AN INFINITE TIMOSHENKO BEAM ON A VISCOELASTIC FOUNDATION TO A HARMONIC MOVING LOAD

Y.-H. CHEN

Civil Engineering and Naval Architecture, National Taiwan University, Taipei, Taiwan, Republic of China

Y.-H. HUANG

Chung-Shun Institute of Science and Technology, Lung-Tan, Taiwan, Republic of China

AND

C.-T. SHIH

Department of Naval Architecture and Ocean Engineering, National Taiwan University, Taipei, Taiwan, Republic of China

(*Received* 26 *October* 1999, *and in final form* 5 *September* 2000)

The dynamic stiffness matrix of an infinite Timoshenko beam on viscoelastic foundation to a harmonic moving load is established. This dynamic stiffness matrix is essentially a function of the velocity and frequency of the harmonic moving load. The critical velocities and the resonant frequencies can be easily determined. The dynamic responses of a European high-speed railway subjected to a harmonic moving load are calculated as an example for demonstration and discussion.

1. INTRODUCTION

The general dynamic stiffness matrix of a finite Timoshenko beam on viscoelastic foundation for engineering applications has been well established [1–9]. It is probably the simplest and the most convenient way to deal with the dynamic behavior of a distributed-parameter beam or beam system described in the continuous-co-ordinate system. Recently, this technique has been extended to an infinite or semi-infinite Timoshenko beam on viscoelastic foundation in order to study the dynamic response of a railway to a constant moving load [10]. There are only two degrees of freedom of displacement involved in the analysis of an infinite or semi-infinite beam on viscoelastic foundation to the moving load; therefore, the dynamic-stiffness method is much more simple and straightforward than any other mathematical procedure [11–22]. In some practical cases [14–16], the moving load cannot be considered constant, the harmonic component of the moving load could be important and should be taken into account in the structural analysis, especially when the loading frequency coincides with the resonant frequency of the railway. This is the purpose of this paper to establish the dynamic stiffness matrix of an infinite or semi-infinite Timoshenko beam on viscoelastic foundation to the harmonic moving load for the railway engineering application.

0022-460X/01/150809 + 16 $35.00/0

2. GOVERNING EQUATION

An infinite Timoshenko beam on viscoelastic foundation is shown in Figure 1. The forces and the deformations of a differential beam element are shown in Figure 2. The governing equations for this case in the fixed co-ordinate system assigned as x and y have been derived and given as follows [1]:

$$m\ddot{y} + c_d\dot{y} + k_s y - k'AG\left[\left(1 - \frac{N}{k'AG}\right)\frac{\partial^2 y}{\partial x^2} - \frac{\partial \alpha}{\partial x}\right] = 0, \tag{1}$$

$$EI\,\frac{\partial^2 \alpha}{\partial x^2} + k'AG\left(\frac{\partial y}{\partial x} - \alpha\right) - J\ddot{\alpha} = 0. \tag{2}$$

All the symbols shown in Figures 1 and 2 and given in equations (1) and (2) are defined as follows; y, β, and α represent the deflection, shear distortion, and bending rotation of the beam; m and J represent the mass and rotary inertia of the mass per unit length of the beam; $k'A$ and I represent the effective shear area and the second moment of area of the beam

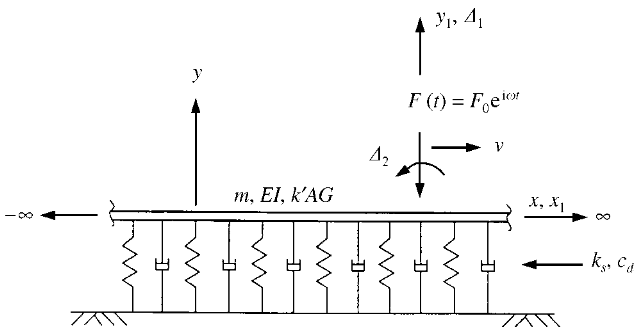

Figure 1. An infinite beam on viscoelastic foundation.

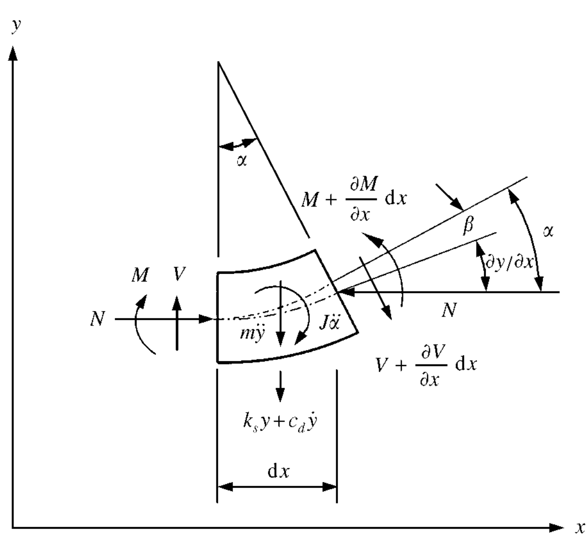

Figure 2. A differential beam element.

section; E and G represent the Young's and shear moduli of the beam; k_s and c_d represent the coefficients of the foundation stiffness and viscous damping per unit length of the beam; N, V, and M represent the constant axial force, shear force, and bending moment at any beam section respectively.

If another co-ordinate system assigned as x_1 and y_1 moving with a harmonic load F travelling rightward at a constant speed v is also shown in Figure 1. The relationship between these two co-ordinate systems are given as

$$x_1 = x - vt, \qquad y_1 = y, \qquad \alpha_1 = \alpha, \tag{3}$$

where t represents the travelling time of the moving co-ordinate system (or the harmonic moving load F), y_1 and α_1 also represents the deflection and rotation of the beam respectively.

Applying the chain rule gives the following results:

$$\frac{\partial y}{\partial x} = \frac{\partial y_1}{\partial x_1}, \qquad \frac{\partial^2 y}{\partial x^2} = \frac{\partial^2 y_1}{\partial x_1^2}, \qquad \frac{\partial y}{\partial t} = \frac{\partial y_1}{\partial t} - v\,\frac{\partial y_1}{\partial x_1}, \qquad \frac{\partial^2 y}{\partial t^2} = \frac{\partial^2 y_1}{\partial t^2} - 2v\,\frac{\partial^2 y_1}{\partial x_1\,\partial t} + v^2\,\frac{\partial^2 y_1}{\partial x_1^2}. \tag{4}$$

The relationships between the derivatives of α and α' have the same results as given in the previous equation. Substituting equations (3) and (4) into equations (1) and (2) can yield the following results:

$$(-k'AG + N + mv^2)\frac{\partial^2 y_1}{\partial x_1^2} - 2mv\frac{\partial^2 y_1}{\partial t\,\partial x_1} + m\frac{\partial^2 y_1}{\partial t^2} - c_d v\frac{\partial y_1}{\partial x_1} + c_d\frac{\partial y_1}{\partial t} + k_s y_1 + k'AG\frac{\partial \alpha_1}{\partial x_1} = 0, \tag{5}$$

$$(-EI + v^2 J)\frac{\partial^2 \alpha_1}{\partial x_1^2} - 2vJ\frac{\partial^2 \alpha_1}{\partial t\,\partial x_1} + J\frac{\partial^2 \alpha_1}{\partial t^2} + k'AG\alpha_1 - k'AG\frac{\partial y_1}{\partial x_1} = 0. \tag{6}$$

The previous equations are the governing equations for the vertical deflection y_1 and the rotation α_1 of a Timoshenko beam on viscoelastic foundation in the moving co-ordinate system x_1 and y_1.

3. COMPLEX WAVE NUMBER

The harmonic moving load can be assumed as $F = F_0\,e^{i\omega t}$, the steady state solutions of equations (5) and (6) could be expressed by

$$y_1 = \Phi(x_1)\,e^{i\omega t}, \qquad \alpha_1 = \Psi(x_1)\,e^{i\omega t}, \tag{7}$$

where $\Phi(x_1)$ and $\Psi(x_1)$ represent the amplitude functions for the deflection $y_1(x_1, t)$ and rotation $\alpha_1(x_1, t)$ respectively. ω represents the frequency of the harmonic moving load.

Substituting equation (7) into equations (5) and (6) and eliminating Φ or Ψ can yield a fourth order ordinary differential equation for Φ or Ψ as follows:

$$\Phi'''' + A_1\Phi''' + a\Phi'' + A_2\Phi' + b\Phi = 0, \quad \Psi'''' + A_1\Psi''' + a\Psi'' + A_2\Psi' + b\Psi = 0. \tag{8}$$

It should be noted that both the fourth order ordinary differential equations for variables Φ and Ψ have the same coefficients A_1, a, A_2, and b given as

$$A_1 = f + g, \qquad A_2 = cg + \frac{bf}{c}, \qquad a = c + \frac{b}{c} + de + fg,$$

$$b = c\,\frac{J\omega^2 - k'AG}{EI - v^2 J}, \qquad c = \frac{m\omega^2 - \mathrm{i}c_d\omega - k_s}{k'AG - N - mv^2},$$

$$d = \frac{k'AG}{k'AG - N - mv^2}, \qquad e = \frac{k'AG}{EI - v^2 J},$$

$$f = \frac{(c_d + \mathrm{i}2m\omega)\,v}{k'AG - N - mv^2}, \qquad g = \frac{\mathrm{i}2J\omega v}{EI - v^2 J}. \tag{9}$$

The solution of equation (8) can be assumed as

$$\Phi(x_1) = \sum_{j=1}^{4} C_j \mathrm{e}^{p_j x_1}, \qquad \Psi(x_1) = \sum_{j=1}^{4} D_j e^{p_j x_1} \tag{10}$$

where p_j represents the complex wave number. The real and imaginary parts of p_j represent the distance decay factor per unit length and the actual wave number of the beam respectively.

The relationship between C_j and D_j can be obtained by substituting equations (7) and (10) into equation (5) or (6) and given as

$$D_j = g_j C_j, \tag{11}$$

where

$$g_j = \frac{p_j}{d}\left(1 + \frac{f}{p_j} + \frac{c}{p_j^2}\right)$$

or

$$g_j = -\frac{e\,p_j}{p_j^2 + g\,p_j + b/c}. \tag{12}$$

Substituting equation (10) into equation (8) yields the equation for the complex wave number p as

$$p^4 + A_1 p^3 + a p^2 + A_2 p + b = 0. \tag{13}$$

If every coefficient of the previous equation is not zero, the four different roots could be assumed as $p_1 = a_1 + \mathrm{i}b_1$, $a_1 \geqslant 0$; $p_2 = a_2 + \mathrm{i}b_2$, $a_2 \leqslant 0$; $p_3 = a_3 + \mathrm{i}b_3$, $a_3 \geqslant 0$; and $p_4 = a_4 + \mathrm{i}b_4$, $a_4 \leqslant 0$.

4. DYNAMIC STIFFNESS MATRIX

The case of $x_1 \geqslant 0$ for a positive-semi-infinite beam as shown in Figure 3(b), C_1, C_3, D_1 and D_3 in equation (10) must be all zero due to the fact that there is no deflection or rotation at $x = \infty$. The deflection and rotation at $x_1 = 0$ assigned as Δ_1 and Δ_2 are the two degrees of freedom of the displacements of this semi-infinite beam. Equation (10) can be rewritten in a matrix form as

$$\begin{Bmatrix} \Phi(0) \\ \Psi(0) \end{Bmatrix} \equiv \begin{Bmatrix} \Delta_1 \\ \Delta_2 \end{Bmatrix} = \begin{bmatrix} 1 & 1 \\ g_2 & g_4 \end{bmatrix} \begin{Bmatrix} C_2 \\ C_4 \end{Bmatrix} \tag{14}$$

or expressed in a simple form as

$$\{\Delta\} = [\mathbf{P}^+]\,\{\mathbf{C}^+\}. \tag{15}$$

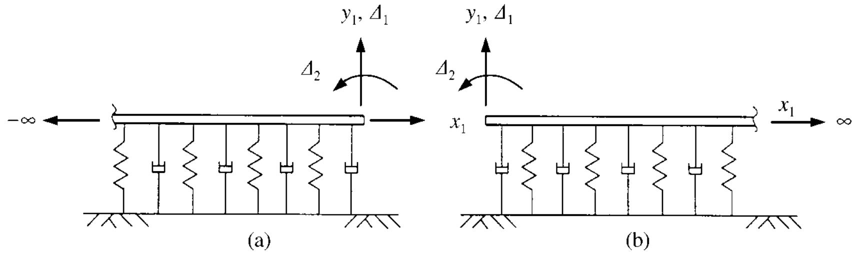

Figure 3. (a) A negative and (b) a positive-semi-infinite beams on viscoelastic foundation.

The corresponding nodal forces, which are the shear force and bending moment at $x_1 = 0$, are given by

$$\{\mathbf{F}^+\} \equiv \begin{Bmatrix} V_1(0) \\ -M_1(0) \end{Bmatrix} = \begin{Bmatrix} k'AG[\Psi(0) - \Phi'(0)] \\ -EI\,\Psi'(0) \end{Bmatrix} + \begin{Bmatrix} N\Phi'(0) \\ 0 \end{Bmatrix} \tag{16}$$

or

$$\{\mathbf{F}^+\} = [\mathbf{L}_1 + \mathbf{L}_2]\,\{\mathbf{C}^+\}, \tag{17}$$

where

$$[\mathbf{L}_1] = \begin{bmatrix} k'AG(g_2 - p_2) & k'AG(g_4 - p_4) \\ -EIp_2g_2 & -EIp_4g_4 \end{bmatrix},$$

$$[\mathbf{L}_2] = N\begin{bmatrix} p_2 & p_4 \\ 0 & 0 \end{bmatrix}. \tag{18}$$

Substituting equation (15) into equation (17), the relationship between the nodal forces and nodal displacements at the left end ($x_1 = 0$) of a positive-semi-infinite Timoshenko beam on viscoelastic foundation can be obtained as

$$\{\mathbf{F}^+\} = [\mathbf{K}^+]\,\{\Delta\}, \tag{19}$$

where

$$[\mathbf{K}^+] = [\mathbf{L}_1 + \mathbf{L}_2]\,[\mathbf{P}^+]^{-1}. \tag{20}$$

$[\mathbf{K}^+]$ represents the dynamic stiffness matrix for a positive-semi-infinite beam ($x_1 \geqslant 0$). The details of $[\mathbf{K}^+]$ are given as follows:

$$K_{11}^+ = \frac{(k'AG - N)(p_4g_2 - p_2g_4)}{g_4 - g_2},$$

$$K_{12}^+ = \frac{(k'AG - N)(p_2 - p_4) - k'AG(g_2 - g_4)}{g_4 - g_2},$$

$$K_{21}^+ = \frac{-EIg_2g_4(p_2 - p_4)}{g_4 - g_2},$$

$$K_{22}^+ = \frac{-EI(p_4g_4 - p_2g_2)}{g_4 - g_2}. \tag{21}$$

The case of ($x_1 \leqslant 0$) for a negative-semi-infinite beam as shown in Figure 3(a), C_2, C_4, D_2 and D_4 in equation (10) must be all zero due to the fact that there is no deflection or rotation at $x = -\infty$. Following the same procedure as to formulate the dynamic stiffness matrix for a positive-semi-infinite beam ($x_1 \geqslant 0$), the dynamic stiffness matrix $[\mathbf{K}^-]$ for a negative-semi-infinite beam ($x_1 \leqslant 0$) can be obtained as follows:

$$K_{11}^- = \frac{(k'AG - N)(p_3 g_1 - p_1 g_3)}{g_1 - g_3},$$

$$K_{12}^- = \frac{(k'AG - N)(p_1 - p_3) - k'AG(g_1 - g_3)}{g_1 - g_3},$$

$$K_{21}^- = \frac{-EIg_1 g_3 (p_1 - p_3)}{g_1 - g_3},$$

$$K_{22}^- = \frac{-EI(p_3 g_3 - p_1 g_1)}{g_1 - g_3}. \tag{22}$$

The deflection and rotation at the origin ($x_1 = 0$) in the moving co-ordinate system are assigned as the two degrees of freedom of the displacement, the dynamic stiffness matrix for an infinite Timoshenko beam on viscoelastic foundation can be achieved by

$$[\mathbf{K}] = [\mathbf{K}^+] + [\mathbf{K}^-]. \tag{23}$$

All the stiffness coefficients are functions of the velocity and frequency of the harmonic moving load F. It is interesting to note that the dynamic stiffness matrix given by equation (23) is also valid for the constant moving load (i.e., $\omega = 0$) or for the static case (i.e., $\omega = 0$ and $v = 0$). In general $[\mathbf{K}^+]$, $[\mathbf{K}^-]$, and $[\mathbf{K}]$ are not symmetrical, but they can become symmetrical when $v = 0$. Furthermore, the stiffness matrix $[\mathbf{K}]$ becomes a diagonal one, all the off-diagonal terms are zero.

5. SHAPE FUNCTION AND DISPLACEMENT WAVE

The coefficients C_j's ($j = 1$–4) can be expressed in terms of the nodal displacements at the origin ($x_1 = 0$) as

$$\{\mathbf{C}^+\} = \begin{Bmatrix} C_2 \\ C_4 \end{Bmatrix} = [\mathbf{Q}^+]\,\{\Delta\},$$

$$\{\mathbf{C}^-\} = \begin{Bmatrix} C_1 \\ C_3 \end{Bmatrix} = [\mathbf{Q}^-]\,\{\Delta\}, \tag{24}$$

where

$$[\mathbf{Q}^+] = [\mathbf{P}^+]^{-1} = \frac{1}{g_4 - g_2}\begin{bmatrix} g_4 & -1 \\ -g_2 & 1 \end{bmatrix},$$

$$[\mathbf{Q}^-] = [\mathbf{P}^-]^{-1} = \frac{1}{g_3 - g_1}\begin{bmatrix} g_3 & -1 \\ -g_1 & 1 \end{bmatrix}. \tag{25}$$

The deflection $\Phi(x_1)$ and rotation $\Psi(x_1)$ given by equation (10) can be rewritten in terms of the nodal displacements Δ_1 and Δ_2 as follows:

$$\Phi(x_1) = \phi_1 \Delta_1 + \phi_2 \Delta_2, \qquad \Psi(x_1) = \psi_1 \Delta_1 + \psi_2 \Delta_2, \tag{26}$$

where ϕ_1, ϕ_2, ψ_1, and ψ_2 are defined as the shape functions given as

$$\begin{aligned}
\phi_1 &= (g_4 e^{p_2 x_1} - g_2 e^{p_4 x_1})/(g_4 - g_2), \quad x_1 \geqslant 0,\\
&= (-g_3 e^{p_1 x_1} + g_1 e^{p_3 x_1})/(g_1 - g_3), \quad x_1 \leqslant 0,\\
\phi_2 &= (-e^{p_2 x_1} + e^{p_4 x_1})/(g_4 - g_2), \quad x_1 \geqslant 0,\\
&= (e^{p_1 x_1} - e^{p_3 x_1})/(g_1 - g_3), \quad x_1 \leqslant 0,\\
\psi_1 &= g_2 g_4 (e^{p_2 x_1} - e^{p_4 x_1})/(g_4 - g_2), \quad x_1 \geqslant 0,\\
&= g_1 g_3 (-e^{p_1 x_1} + e^{p_3 x_1})/(g_1 - g_3), \quad x_1 \leqslant 0,\\
\psi_2 &= (-g_2 e^{p_2 x_1} + g_4 e^{p_4 x_1})/(g_4 - g_2), \quad x_1 \geqslant 0,\\
&= (g_1 e^{p_1 x_1} - g_3 e^{p_3 x_1})/(g_1 - g_3), \quad x_1 \leqslant 0.
\end{aligned} \tag{27}$$

6. CRITICAL VELOCITY AND RESONANT FREQUENCY

The dynamic stiffness matrix of an infinite Timoshenko beam on viscoelastic foundation to a harmonic moving load is established in this paper and given by equation (23). All the dynamic stiffness coefficients are functions of the velocity and frequency of the harmonic moving load. The determinant of this dynamic stiffness matrix could be zero at certain velocities and frequencies for an undamped case, i.e.,

$$|\mathbf{K}(v, \omega)| = 0. \tag{28}$$

Equation (28) gives the resonant condition, by which the critical velocities and the resonant frequencies can be determined. If $\omega = 0$, equation (28) becomes a function of velocity only, the velocity which satisfies this condition is called the critical velocity for an undamped infinite Timoshenko beam on elastic foundation to a constant moving load. If $v = 0$, equation (28) can also give the natural frequency for an undamped infinite Timoshenko beam on elastic foundation, and it is exactly equal to that of a simple spring–mass system, i.e., $\omega_n = (k_s/m)^{1/2}$.

7. EXAMPLE AND DISCUSSION

A European high-speed rail as shown in Figure 4 has the following properties: $A = 76{\cdot}86\ \mathrm{cm}^2$, $I = 3{\cdot}06 \times 10^3\ \mathrm{cm}^4$, $m = 60{\cdot}34$ kg/m, $E = 2 \times 10^7\ \mathrm{N/cm}^2$, $J = 2{\cdot}41 \times 10^{-1}$ kg m, $k' = 0{\cdot}2$, $v = 0{\cdot}3$, $G = 7{\cdot}69 \times 10^6\ \mathrm{N/cm}^2$. The influences of the stiffness coefficient of the rail foundation on the critical velocity (v_{cr}) and the resonant frequency (ω_r) of the harmonic moving load are shown in Figures 5 and 6 respectively. It should be noted that the critical velocity of the rail on a specific foundation could have one or two values for a given loading frequency ω. When $\omega = 0$ for the case of a constant moving load, there is only a critical velocity. The two critical velocities approach one as the loading frequency ω approaches zero, and they separate from the critical velocity for $\omega = 0$ more and more as ω increases, one is decreasing and the other is increasing from the critical velocity for $\omega = 0$ respectively. The foundation stiffness $k_s = 1{\cdot}0 \times 10^7\ \mathrm{N/m}^2$ for an example, the critical velocity has two values when $\omega \leqslant 407{\cdot}10$ rad/s, and it has only one value when $\omega > 407{\cdot}10$ rad/s. The critical velocity increases as the foundation stiffness increases for a given loading frequency. Figures 5 and 6 also show the relationship between the critical velocity and the resonant frequency. If the ranges of the foundation stiffness, the velocity

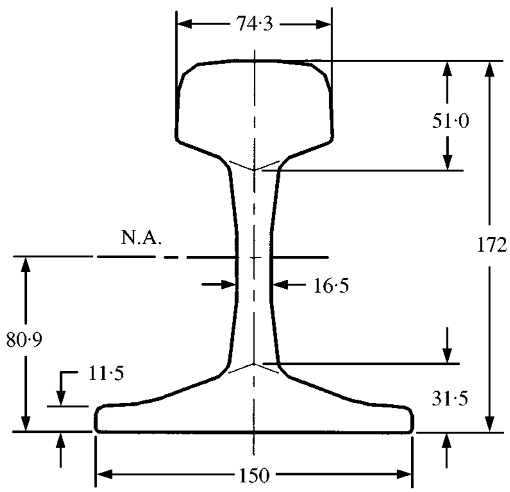

Figure 4. A European high-speed rail (UIC60), unit: mm.

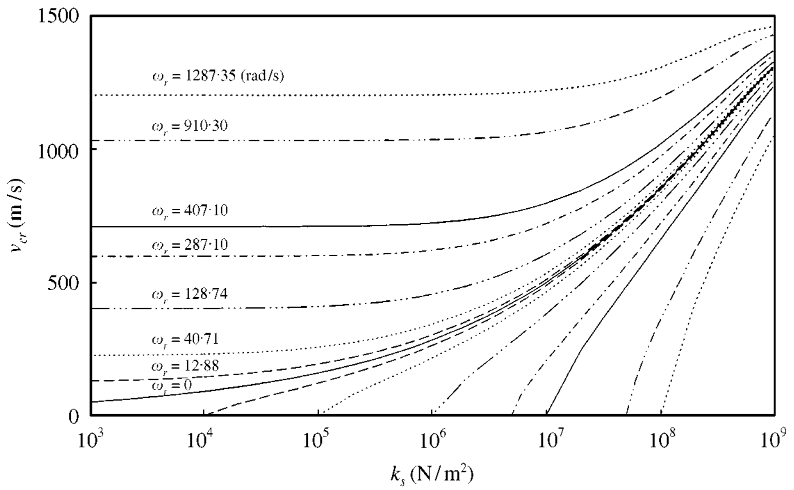

Figure 5. Critical velocity and resonant frequency versus foundation stiffness.

and frequency of the moving load for today's engineering interest are as follows: $5 \times 10^6 \leqslant k_s < 10^9$ N/m^2, $v < 200$ m/s, and $\omega < 4000$ r.p.m.; therefore the resonance of this rail example could not occur in engineering application except $k_s \leqslant 2 \times 10^7$ N/m^2.

The damping ratio of the rail system is defined by $\xi = c_d/c_{cr}$, where c_{cr} represents the critical damping coefficient defined by $c_{cr} = 2(m\ k_s)^{1/2}$. The given rail on the viscoelastic foundation of $k_s = 1{\cdot}6 \times 10^7$ N/m^2, and $\xi = 0$–$0{\cdot}8$ are under investigation. The determinant and coefficients of the dynamic stiffness matrix are shown in Figures 7 and 8 for the loading frequencies $\omega = 0$ and 400 rad/s respectively. All the imaginary parts of the stiffness coefficients for $\omega = 0$ are very small and can be neglected. There is only one critical velocity at $v_{cr} = 558{\cdot}94$ m/s for $\omega = 0$,. and there are two critical velocities at $v_{cr} = 189{\cdot}77$ and 821·40 m/s for $\omega = 200$ rad/s. The real parts of all the stiffness coefficients for $\xi = 0$ and $\omega = 0$ are zero at the critical velocity $v_{cr} = 558{\cdot}94$ m/s, but only the real or imaginary parts

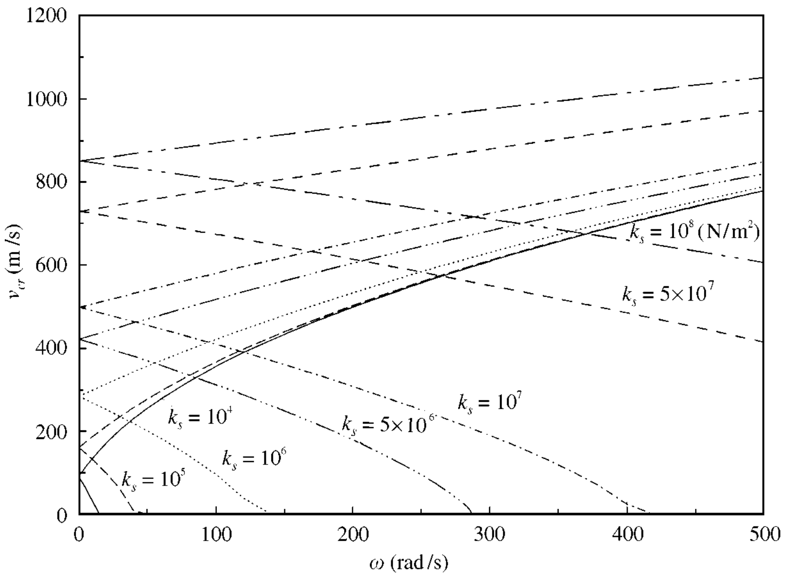

Figure 6. Critical velocity versus resonant frequency for different foundation stiffness.

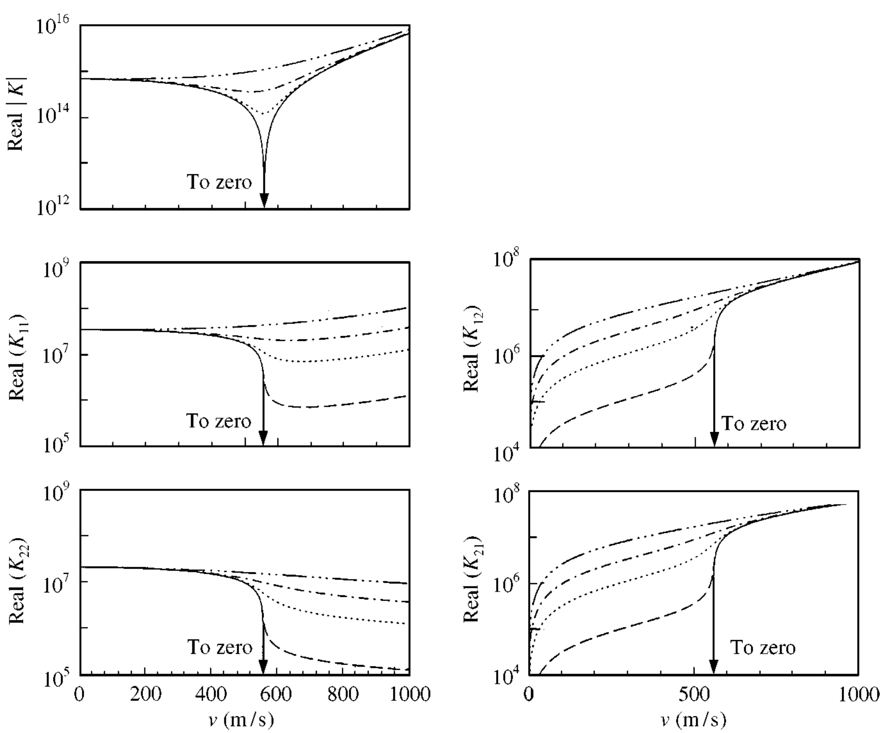

Figure 7. Dynamic stiffness matrix for constant moving load ($\omega = 0$, $v_{cr} = 558{\cdot}94$ m/s): ——, $\xi = 0$; – – – – –, $\xi = 0{\cdot}01$; ...., $\xi = 0{\cdot}1$; –·–·–·, $\xi = 0{\cdot}3$; — ···— ···, $\xi = 0{\cdot}8$.

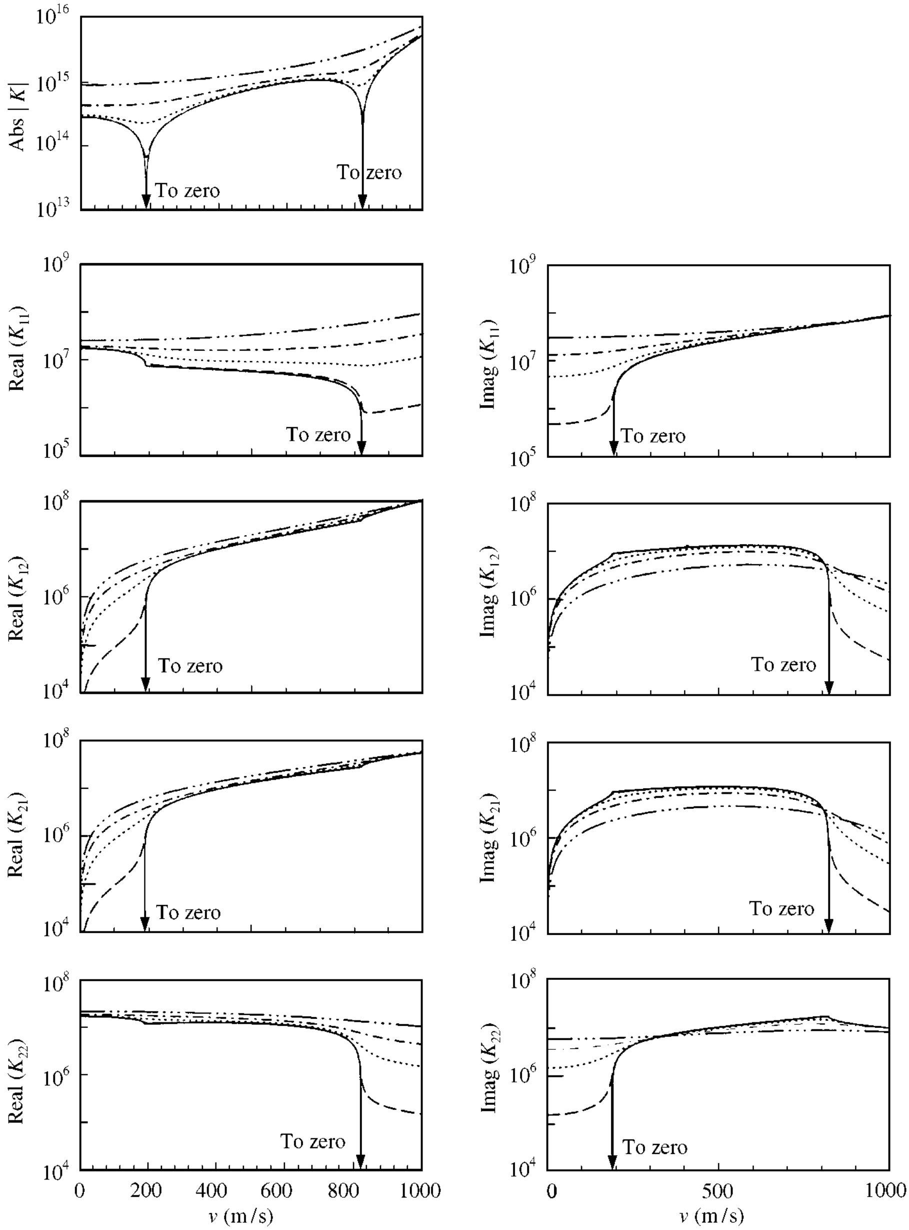

Figure 8. Dynamic stiffness matrix for harmonic moving load ($\omega = 400$ rad/s, $v_{cr} = 189{\cdot}77$ and $821{\cdot}40$ m/s): ——, $\xi = 0$; – – – –, $\xi = 0{\cdot}01$; ...., $\xi = 0{\cdot}1$; — · — · —, $\xi = 0{\cdot}3$; — · · · — · · ·, $\xi = 0{\cdot}8$.

of the stiffness coefficients for $\xi = 0$ and $\omega \neq 0$ are zero at the two critical velocities $v_{cr} = 189{\cdot}77$ and $821{\cdot}40$ m/s.

The shape functions $\phi_1(x_1)$ and $\phi_2(x_1)$ of the rail are shown in Figure 9 for the cases of $v = 200$ m/s, $\omega/\omega_r = 0$–$4{\cdot}0$ (where $\omega_r = 391{\cdot}52$ rad/s), and $\xi = 0{\cdot}1$. The amplitude functions of the deflection $\Phi(x_1)$, rotation $\Psi(x_1)$, bending moment $M(x_1)$, and shear force $V(x_1)$ of the rail subjected to a harmonic moving load $F(t) = F_0\, e^{i\omega t}\, \delta(x - vt)$, where $F_0 = -10$ kN and $v = 200$ m/s, are as shown in Figures 10 and 11 respectively. The phase angle of the

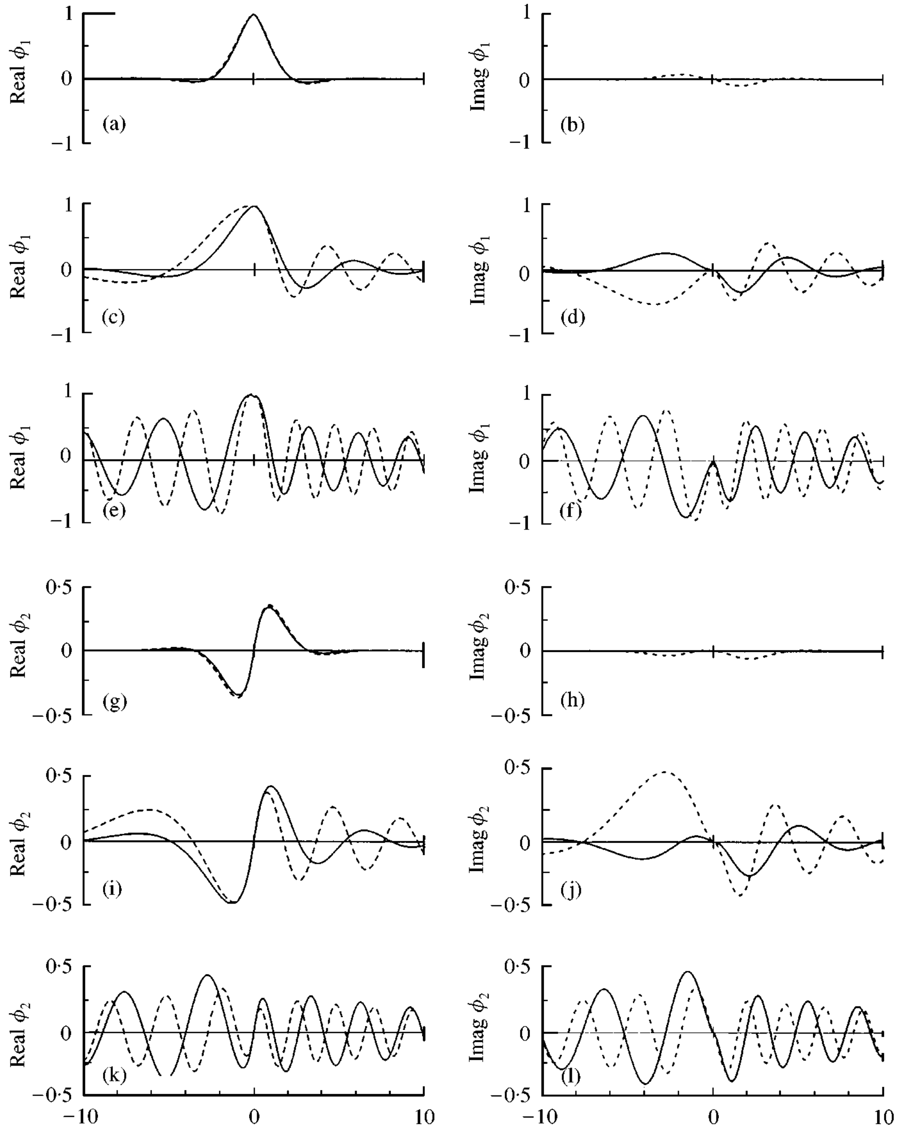

Figure 9. Shape functions ($v = 200$ m/s, $\omega_r = 391{\cdot}52$ rad/s, $\xi = 0{\cdot}1$). (a, b, g, h) ——, $\omega/\omega_r = 0$, ----, $\omega/\omega_r = 0{\cdot}5$; (c, d, i, j) ——, $\omega/\omega_r = 1{\cdot}0$, ----, $\omega/\omega_r = 1{\cdot}5$; (e, f, k, l) ——, $\omega/\omega_r = 2{\cdot}5$, ---- $\omega/\omega_r = 4.0$.

displacement (or stress) wave at each point x_1 could be different due to the damping presented in the rail system. It means that the different positions on the rail could not be vibrating at the same phase. All the imaginary parts of the displacement (or stress) waves as shown in Figures 9–11 should be vanished for an undamped system (i.e., $\xi = 0$). For the case of $\omega/\omega_r < 0{\cdot}5$, the dynamic effect becomes less and less important, and the rail response approaches the static one as ω/ω_r approaches zero. Therefore, all the imaginary parts of the displacement waves as shown in Figures 9 and 10 are small and could be neglected for the low-frequency cases (say $\omega/\omega_r \leqslant 0{\cdot}5$). The wave shapes of these low-frequency cases

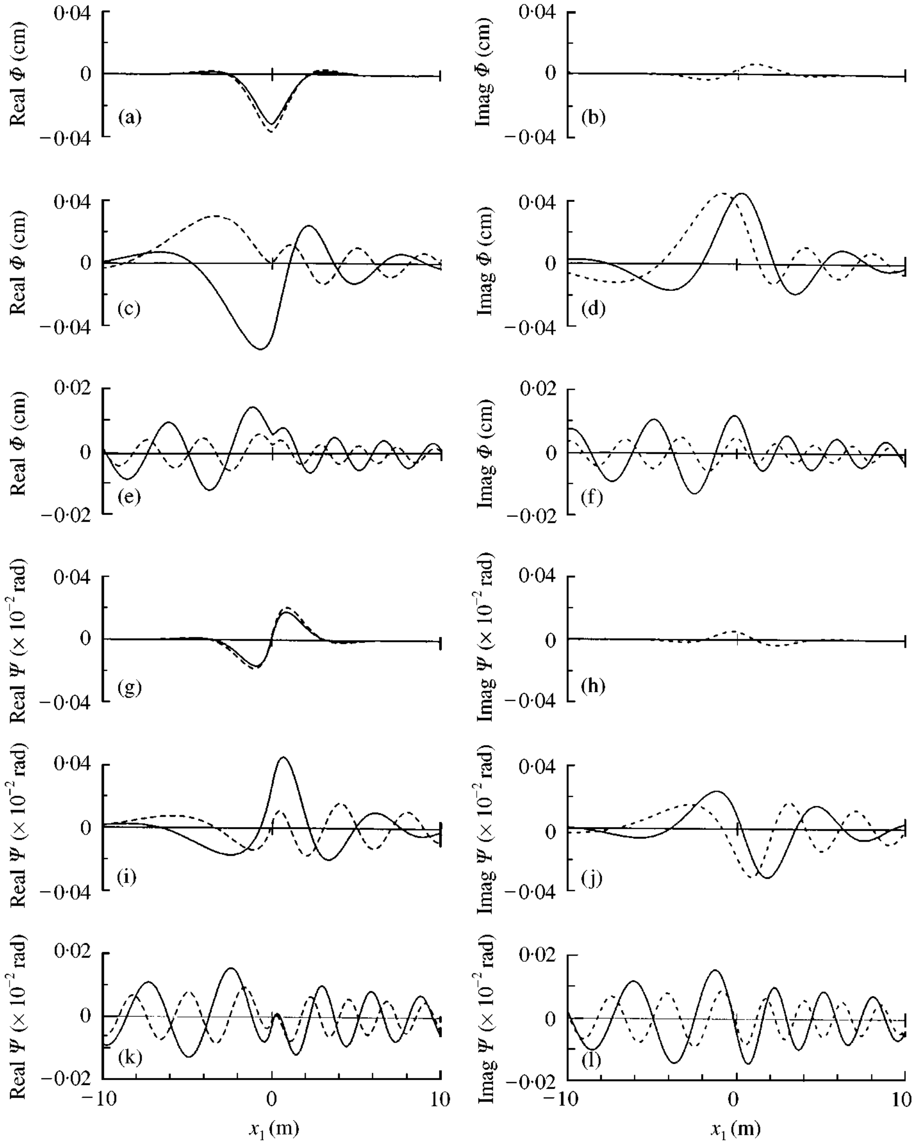

Figure 10. Real and imaginary parts of amplitudes of deflection and rotation ($v = 200$ m/s, $\omega_r = 391{\cdot}52$ rad/s, $\xi = 0{\cdot}1$). (a, b, g, h) ——, $\omega/\omega_r = 0$, - - - -, $\omega/\omega_r = 0{\cdot}5$; (c, d, i, j) ——, $\omega/\omega_r = 1{\cdot}0$, - - - -, $\omega/\omega_r = 1{\cdot}5$; (e, f, k, l) ——, $\omega/\omega_r = 2{\cdot}5$, - - - - $\omega/\omega_r = 4.0$.

are very similar to that for the case of $\omega = 0$, and they are almost symmetrical or antisymmetrical about the loading point for these cases. As $\omega/\omega_r > 0{\cdot}5$, the dynamic effect become more and more important, and the damping ratio will play an important role for these cases. Both the real and imaginary parts of the displacement wave become smaller and smaller as $\omega/\omega_r \geqslant 2{\cdot}0$. All the waves die out very fast as the distance x_1 increases from the loading point also for the low-frequency cases, on the contrary they could propagate longer distance away from the loading point for the high-frequency cases (say $\omega/\omega_r \geqslant 1{\cdot}0$). The length of the front waves are smaller than that of the rear ones for these high-frequency cases. The deflection and stress are significant when the loading frequency coincides with

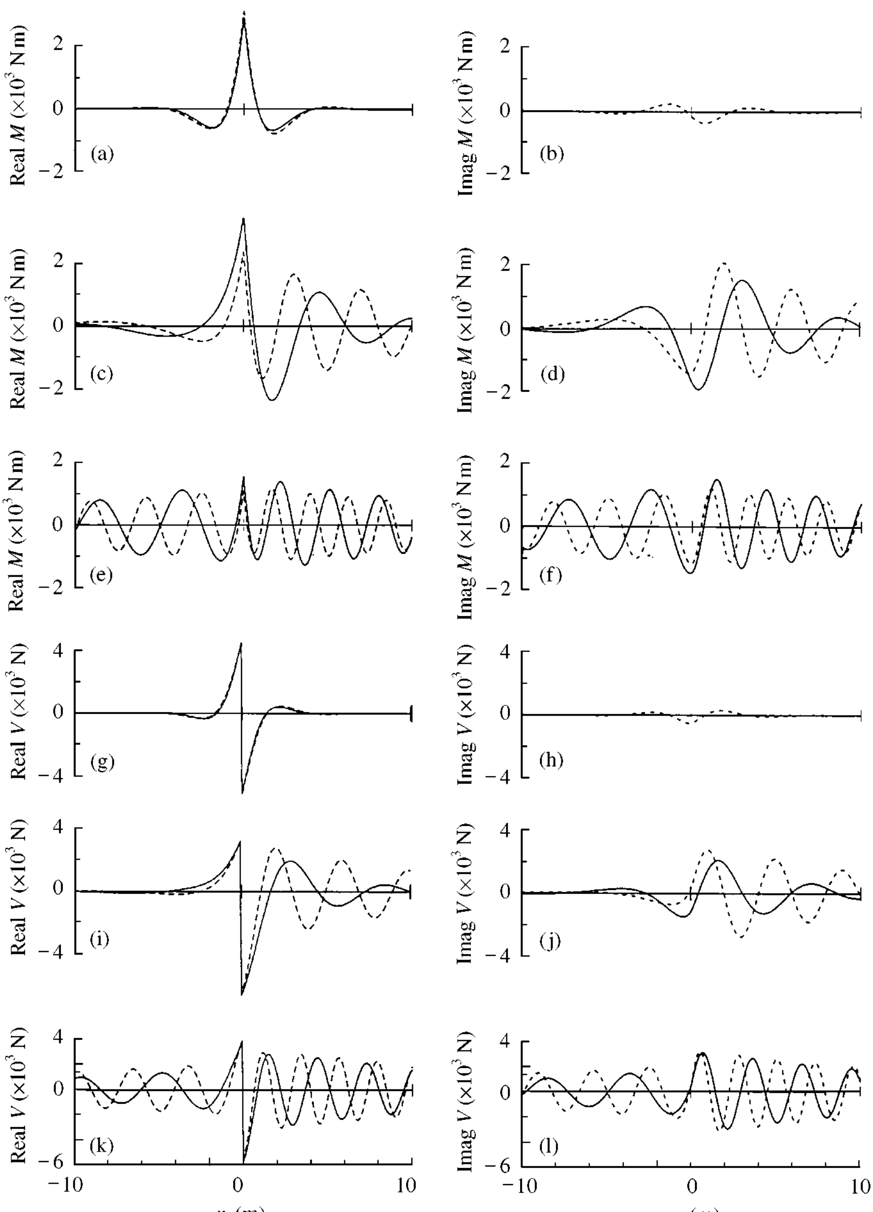

Figure 11. Real and imaginary parts of amplitudes of bending moment and shear force ($v = 200$ m/s, $\omega_r = 391{\cdot}52$ rad/s, $\xi = 0{\cdot}1$). (a, b, g, h) ——, $\omega/\omega_r = 0$, - - - -, $\omega/\omega_r = 0{\cdot}5$; (c, d, i, j) ——, $\omega/\omega_r = 1{\cdot}0$, - - - -, $\omega/\omega_r = 1{\cdot}5$; (e, f, k, l) ——, $\omega/\omega_r = 2{\cdot}5$, - - - - $\omega/\omega_r = 4.0$.

the resonant frequency, i.e., $\omega = \omega_r$, especially for the low damping case. The phase angle θ and amplitude A of the displacement (or stress) wave at any position x_1 can be obtained by $\tan\theta = I/R$ and $A = (R^2 + I^2)^{1/2}$, where R and I represent the real and imaginary parts of the displacement (or stress) wave at the position x_1 respectively. The phase angle and amplitude of the deflection (or stress) wave of the rail example subjected the harmonic moving load at resonance (i.e., $\omega/\omega_r = 1{\cdot}0$) are shown in Figure 12. The amplitude of the

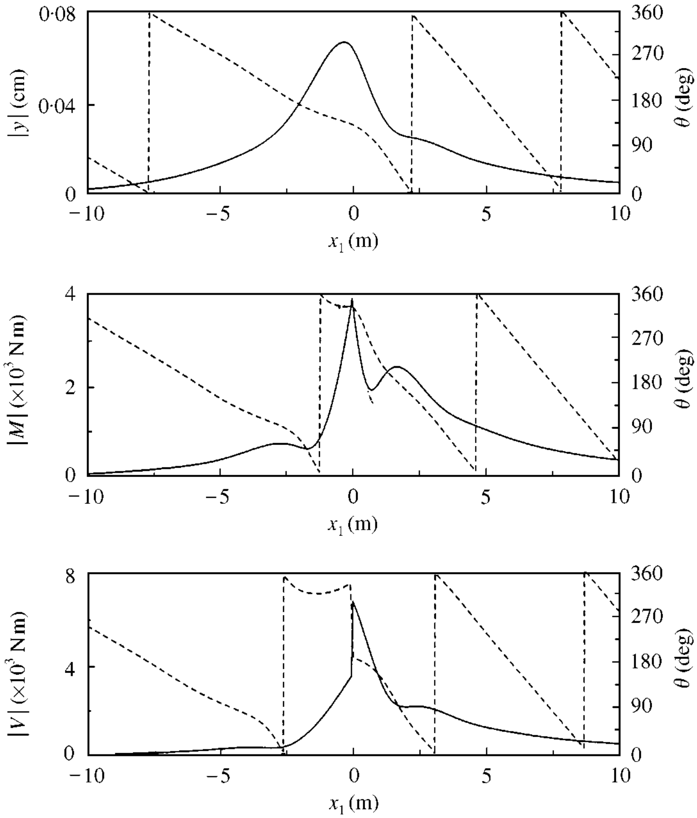

Figure 12. Phase angles and amplitudes of deflection, bending moment, and shear force ($v = 200$ m/s, $\omega_r = 391{\cdot}52$ rad/s, $\xi = 0{\cdot}1$, $\omega/\omega_r = 1{\cdot}0$): ———, amplitude; - - - - - - -, phase angle.

front deflection wave at resonance is almost the same as the rear one. But the amplitude of the front stress waves are much larger than that of the rear ones. It can also be seen obviously from the phase-angle curve in Figure 12 that the front wavelength of the deflection or stress is smaller than the rear one.

8. CONCLUSIONS

Some conclusions could be drawn from this study and given as follows:

(1) The dynamic stiffness matrix established in this paper is simple and very efficient to be applied to the analysis of an infinite or semi-infinite Timoshenko beam on viscoelastic foundation to a harmonic moving load. It can also be applied to a harmonic load ($v = 0$) or a constant moving load ($\omega = 0$) as a special cases.

(2) The dynamic stiffness matrix is essentially a function of the velocity and the frequency of the harmonic moving load. Therefore, the critical velocity and resonant frequency can be easily determined by setting the determinant of the dynamic stiffness matrix equal to zero

(3) There is only one critical velocity for the case of a constant moving load ($\omega = 0$), but there might be one or two critical velocities for the case of a harmonic moving load ($\omega \neq 0$).

(4) The two critical velocities approach one as the loading frequency ω approaches zero, and they separate from the critical velocity for $\omega = 0$ more and more as ω increases, one is decreasing and the other is increasing from the critical velocity for $\omega = 0$ respectively.

(5) The dynamic response due to the harmonic component of a moving load might be important and should be taken into account in analysis, especially for the low-damping case and when the loading frequency (ω) coincides with the resonant frequency (ω_r).

(6) The imaginary parts of the shape functions and the amplitude functions of the deflection, rotation, bending moment, and shear force are all very small and could be neglected for the low-frequency cases (say $\omega/\omega_r \leqslant 0{\cdot}5$).

(7) The wave shapes of the responses for the low-frequency cases (say $\omega/\omega_r \leqslant 0{\cdot}5$) are very similar to that for the case of the constant moving load ($\omega = 0$), and they are almost symmetrical (for the deflection and bending moment) or antisymmetrical (for shear force) about the loading point for these cases.

(8) All the response waves die out very fast as the distance x_1 increases from the loading point for the low-frequency cases (say $\omega/\omega_r \leqslant 0.5$), but they could propagate longer distance away from the loading point for the high-frequency cases (say $\omega/\omega_r \geqslant 1{\cdot}0$).

(9) The length of the front waves of the responses are smaller than that of the rear waves for the high-frequency cases (say $\omega/\omega_r \geqslant 1{\cdot}0$).

(10) As $\omega/\omega_r > 0{\cdot}5$, the dynamic effect becomes more and more important, and the damping ratio will play an important role for these case. Both the real and imaginary parts of the deflection wave become smaller and smaller as $\omega/\omega_r \geqslant 2{\cdot}0$.

ACKNOWLEDGMENTS

The authors gratefully acknowledge the sponsorship of this study from National Taiwan University and the National Science Council of the Republic of China.

REFERENCES

1. Y.-H. Chen 1987 *Earthquake Engineering and Structural Dynamics* **15**, 391–402. Generalized dynamic-stiffness matrix of a Timoshenko beam for transverse vibration.
2. Y.-H. Chen 1988 *Journal of Ship Research*, *SNAME*, **32**, 177–185. General dynamic shape function and stiffness matrix and their application to structural-borne noise on ships.
3. Y.-H. Chen and I. M. Bertran 1990 *International Shipbuilding Progress* **37**, 151–163. Parametric study of ship–hull vibration.
4. Y.-H. Chen and J.-T. Sheu 1993 *International Journal for Numerical Methods in Engineering* **36**, 1013–1027. Axially-loaded damped Timoshenko beam on viscoelastic foundation.
5. Y.-H. Chen and J.-T. Sheu 1994 *Journal of Vibration and Acoustics*, *American Society of Mechanical Engineers* **116**, 350–356. Dynamic characteristics of layered beam with flexible core.
6. Y.-H. Chen and J.-T. Sheu 1995 *Journal of Engineering Mechanics*, *American Society of Civil Engineers* **121**, 340–344. Beam on viscoelastic foundation and layered beam.
7. Y.-H. Chen and J.-T. Sheu 1996 *Computer Methods in Applied Mechanics and Engineering* **129**, 311–318. Beam length and dynamic stiffness.
8. Y.-H. Chen and C.-Y. Lin 1998 *Journal of Sound and Vibration* **212**, 759–769. Structural analysis and optimal design of a dynamic absorbing beam.
9. Y.-H. Chen and C.-Y. Li 2000 *Journal of Bridge Engineering*, *American Society of Civil Engineers* **5**, 124–130. Dynamic response of elevated high-speed railway.
10. Y.-H. Chen and Y.-H. Huang 2000 *International Journal for Numerical Methods in Engineering* **48**, 1–18. Dynamic stiffness of infinite Timoshenko beam on viscoelastic foundation in moving coordinate.

11. H. E. Criner and G. D. McCann 1953 *Journal of Applied Mechanics*, *American Society of Mechanical Engineers* **75**, 13–22. Rails on elastic foundation under the influence of high-speed travelling loads.
12. J. T. Kenney Jr 1954 *Journal of Applied Mechanics*, *American Society of Mechanical Engineers* **76**, 359–364. Steady-state vibrations of beam on elastic foundation for moving load.
13. J. D. Achenbach and C. T. Sun 1965 *International Journal of Solids and Structures*, **1,** 353–370. Moving load on a flexible supported Timoshenko beam.
14. R. A. Clark, P. A. Dean, J. A. Elkins and S. G. Newton 1982 *Journal of Mechanical Engineering Science* **24**, 65–76. An investigation into the dynamic effects of railway vehicles running on corrugated rail.
15. S. L. Grassie, R. W. Gregory, D. Harrison and K. L. Johnson 1982 *Journal of Mechanical Engineering Science* **24**, 77–90. The dynamic response of railway track to high frequency vertical excitation.
16. S. L. Grassie, R. W. Gregory and K. L. Johnson 1982 *Journal of Mechanical Engineering Science* **24**, 103–111. The behavior of railway wheelsets and track at high frequencies of excitation.
17. A. M. Trochanis, R. Chelliah and J. Bielak 1987 *Journal of Geotechnical Engineering*, *American Society of Civil Engineers* **113**, 879–895. Unified approach for beams on elastic foundations under moving loads.
18. Y.-H. Lin and M. W. Trethewey 1990 *Journal of Sound and Vibration* **136**, 323–342. Finite element analysis of elastic beams subjected to moving dynamic loads.
19. Z. Cai and G. P. Raymond 1994 *Structural Engineering and Mechanics* **2**, 95–112. Modelling the dynamic response of railway track of wheel/rail impact loading.
20. D. Thambiratnam and Y. Zhuge 1996 *Journal of Sound and Vibration* **198**, 149–169. Dynamic analysis of beams on an elastic foundation subjected to moving loads.
21. S. F. Felszeghy 1996 *Journal of Vibration and Acoustics*, *American Society of Mechanical Engineers* **118**, 277–284. The Timoshenko beam on an elastic foundation and subjected to a moving step load, Part 1: steady-state response.
22. S. F. Felszeghy 1996 *Journal of Vibration and Acoustics*, *American Society of Mechanical Engineers* **118**, 285–291. The Timoshenko beam on an elastic foundation and subjected to a moving step load, Part 2: transient response.